Computer Simulation of Fractal Dimensions of Fat Crystal Networks

Dongming Tang and Alejandro G. Marangoni*

Department of Food Science, University of Guelph, Guelph, Canada, N1G 2W1

ABSTRACT: The rheological properties of fat-structured products are determined by the microstructure of their fat crystal networks, which can be quantified by using microscopical and rheological techniques. Of particular interest to this study is the quantification of the fractal dimension of the network using these two techniques. Fractal dimensions determined by polarized light microscopy include box-counting, particle-counting, and Fourier-transform fractal dimensions, whereas the fractal dimensions determined by small deformation dynamic rheology exploit the dependence of the storage modulus on the solids' volume fraction. This work reveals that different microscopy fractal dimensions are sensitive to different microstructural factors within the fat crystal network, and thus have different physical meanings. The box-counting fractal dimension, D_b, increases with increases in crystal size and area fraction of the fat crystals, whereas the particle-counting fractal dimension, D_f, is sensitive to the radial distribution pattern of fat crystals; and the Fourier-transform fractal dimension, D_{FT}, decreases with increasing crystal size. In the studies on the macroscopic physical properties of fat crystal networks, it is necessary to find the determining structural characteristics and then use the fractal dimensions that are most closely related.

Paper no. J11270 in *JAOCS 83,* 309–314 (April 2006).

KEY WORDS: Fat crystal networks, fractal dimensions, simulation.

In food products containing solid fat as the continuous phase, the fat crystals interact with each other to form a 3-D fat crystal network, which percolates throughout the system. The shape, size, number of fat crystals, and the spatial distribution pattern of the fat crystals, which constitute the microstructure of the fat crystal network, are key factors determining the rheological properties of the network and hence the food product. According to the fractal model developed for fat crystal networks by our group (1–3), the microstructure of fat crystal networks is related to their rheological properties through the fractal dimension of the fat crystal networks, D, as:

$$G' = \lambda \Phi^{\frac{1}{3-D}} \quad [1]$$

where G' is the shear storage modulus of the fat samples, Φ is the volume fraction of solids [(SFC/100), where SFC = solid fat content] of the samples, D is the fractal dimension of the fat crystal networks, and λ is the pre-exponential factor, which depends on the size of the microstructural element within the network and the nature of the intermolecular forces.

The fractal dimensions of fat crystal networks can be obtained from rheology experiments (termed rheology fractal dimensions) and from 2-D image analysis of the polarized light microscopy of fat samples (termed microscopy fractal dimensions). To show that the change in the microstructure of the fat crystal networks causes the change in the rheological properties of the fat samples, it is necessary to have consistency between the rheology fractal dimensions and the microscopy fractal dimensions. Furthermore, several methods have been used to calculate the microscopy fractal dimensions including the extensively used box-counting and particle-counting methods (4–9). Moreover, the fractal dimensions calculated by different methods often have different values and even display different trends when the microstructure of the fat crystal networks is changed (7–9). For example, for the same HMF (high melting fraction of milk fat) samples, the measured box-counting fractal dimension, D_b, ranged from 1.75 to 1.87, whereas the values of the particle-counting fractal dimension, D_f, were from 1.92 to 2.10 (8). Different values of D_b and D_f for the same cocoa butter samples were also reported by Awad and Marangoni (9). During the crystallization of HMF at 5°C, D_b did not vary much, but the D_f values of the same samples increased from 1.97 to 2.10 as the concentration of glycerol was increased from 0 to 0.25% (8). In this paper, we have studied how different microstructural factors affect the microscopy fractal dimensions obtained by different methods to reveal their physical meaning, and then used this knowledge to find the microscopy fractal dimensions that most closely resemble the rheology fractal dimension, D_r. Once this is established unambiguously, these microscopy fractal dimensions can then be used to quantify the microstructure of the fat crystal networks and further predict the rheological properties of the fat samples according to the fractal model of fat crystal networks.

The fractal dimension is an intensive property of a fractal object (10). All fractal objects exhibit a self-similar or self-affine character, which means the pattern of the fractal object is repeated at different length scales. The self-similar character of the fat crystal networks was discussed by Narine and Marangoni (4). All the commonly available methods to calculate the microscopy fractal dimensions of the fat crystal networks, such as box-counting, particle-counting, and Fourier-transform method, are based on this self-similar character of the fat crystal networks. Different methods measure different

*To whom correspondence should be addressed at Dept. of Food Science, University of Guelph, 50 Stone Road West, Guelph, Ontario, Canada, N1G 2W1. E-mail: amarango@uoguelph.ca

properties of the fractal object, for instance, the length, area, or volume of the object at different length scales. For an exact self-similar fractal object, the length (or area, volume) has a power-law relationship to the length scale, and the fractal dimension of the object can be derived from the exponential term of this power law relationship.

Box-counting fractal dimension, D_b. To calculate the box-counting fractal dimension, D_b, grids with side length l_i are laid over a threshold binary image of a fat crystal network. The grids containing particles of more than a threshold value *m* are defined as the occupied grids. The number of occupied grids, N_i, is counted for a series of grid side length l_i. Since the fat crystal network is a fractal object, the number of the occupied grids has a power law relationship with the grid side length, so the plot of the $\log(N_i)$ vs. $\log(l_i)$ is linear. The negative of the slope of this log-log plot is the box-counting fractal dimension, D_b, i.e.,

$$D_b = -\frac{\Delta \ln(N_i)}{\Delta \ln(l_i)} \quad [2]$$

Particle-counting fractal dimension, D_f. The particle-counting fractal dimension, D_f, relates the number of primary particles, *N*, that a fractal object contains with the linear size, *R*, of that object according to the equation:

$$N \propto R^{D_f} \quad [3]$$

To calculate the particle-counting fractal dimension, D_f, of a fat crystal network, a square-shaped ROI (Region of Interest) with different side length, *R*, is drawn on the center of the image of the fat samples and the number of the microstructural element in each ROI is counted. The logarithm of the number of microstructural elements, $\ln(N(R))$, is plotted against the logarithm of the side length of each ROI, $\ln(R)$, for varying values of *R*. The slope of the linear regression curve of this log-log plot is the particle-counting fractal dimension, D_f (5). The particle-counting fractal dimension algorithm should be carried out within the range between 100% and 35% of the original image size (4,9).

Fourier-transform fractal dimension, D_{FT}. In image analysis, a 2-D microscopy image is considered to be a discrete function, *f(x,y)*, where *x* and *y* are the coordinates of the object pixels in the horizontal and vertical direction. The 2-D Discrete Fourier Transform is applied to transform the 2-D image to its corresponding power spectrum image *F(u,v)* as:

$$F(u,v) = \frac{1}{MN} \sum_{x=0}^{M-1} \sum_{y=0}^{N-1} f(x,y) * e^{-j*2\pi(ux/M + vy/N)} \quad [4]$$

or, writing in the form of sine and cosine functions, as:

$$F(u,v) = \frac{1}{MN} \sum_{x=0}^{M-1} \sum_{y=0}^{N-1} f(x,y)[\cos(2\pi(ux/M + vy/N)) - j\sin(2\pi(ux/M + vy/N))] \quad [5]$$

where *u* and *v* are the coordinates of the pixels in the frequency domain image. The power spectrum of *F(u,v)* is

$$P(u,v) = |F(u,v)|^2 = R^2(u,v) + I^2(u,v) \quad [6]$$

where R(*u,v*) is the real part of the function F(*u,v*) and I(*u,v*) is the imaginary part. The power spectrum image is the transformed plotting of P(*u,v*) against the *u, v* dimension. Because the values of *u, v* represent the frequency of how the fashion of the fractal object is repeated, and the power (or the magnitude) of the power spectrum image corresponds to the population of the microstructural elements at each repeating frequency (thus at different length scales), then for a fractal object, the logarithm of the power (or the magnitude) in the power spectrum image shows a linear relationship with the logarithm of the frequencies. The slope of this linear relationship β is used to calculate the Fourier-transform fractal dimension D_{FT} by Equation 7 (11):

$$D_{FT} = \frac{4 + \beta}{2} \quad [7]$$

D_{FT} can be used to study both self-similar and self-affine fractal objects. The data at low frequencies (*u* and *v* < 10) are not to be included in the calculation of D_{FT} (11). Figure 1 (7) illustrates how D_b, D_f, and D_{FT} are calculated from the double logarithmic plot of *X* vs. *Y* for the polarized light microscopy images of the fat crystal networks.

From this discussion, it is obvious that different fractal dimensions use different algorithms and thus may have different values even for the same microstructure. During studies on the microstructure of fat crystal networks, our group has compared the fractal dimension of fat samples calculated by different methods (3–5,12). Narine and Marangoni (4) calculated fractal dimensions of CB (cocoa butter), noninterestified milk fat, palm oil, lard, and tallow by particle-counting method and by rheology (weak link regime) method. A good agreement was found between these two fractal dimensions of the samples (4). In the study on the relationship between the crystallization behavior and the microstructure of palm oil-based shortenings, Litwinenko *et al.* (5) found that a high value of D_f is associated with a more orderly distribution of fat crystals in space. On the other hand, a high value of D_b often represents a more space-filling network, which is the result of fast cooling or high degree of supercooling (13). Awad and Marangoni (9) studied D_f and D_b as a function of crystallization temperature for AMF (anhydrous milk fat), MF-DAG (milk fat diacylglycerol), MF-TAG (milk fat triacylglycerol), and CB. D_f and D_b showed similar trends with temperature for CB, but for the rest of the samples, opposite behaviors of D_f and D_b were evident: When the temperature was above 15°C, D_f increased with temperature and D_b decreased. All these results suggest that the microstructure of a fat crystal network can be quantified using a fractal dimension; however, the fractal dimensions calculated by different methods may have different physical meanings and thus reflect different aspects of the microstructure of the fat crystal network.

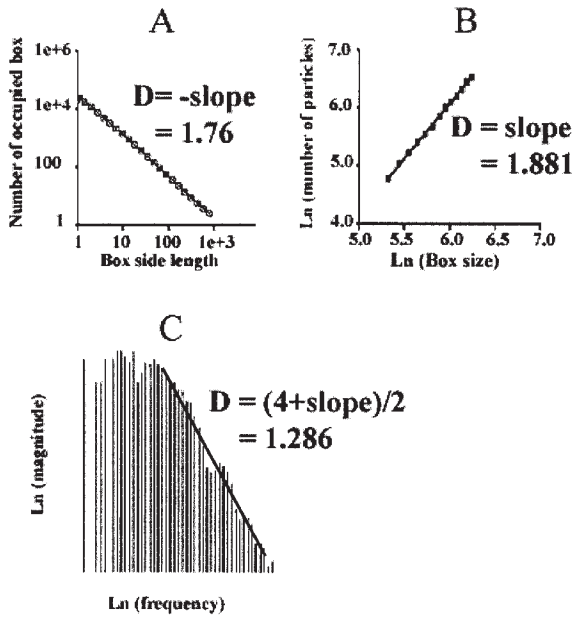

FIG. 1. Illustration of the log-log plot of D_b (box-counting fractal dimension), D_f (particle-counting fractal dimension), and D_{FT} (Fourier-transform fractal dimension). (A) Calculation of D_b; (B) calculation of D_f; (C) calculation of D_{FT}.

When we determine the microscopy fractal dimensions of the fat crystal networks from their polarized light micrographs, the change in the fractal dimensions normally results from the combined effects of several structural factors and it is hard to tell how each individual structural factor affects the value of the fractal dimensions. By using computer simulation, we changed each of the microstructural factors individually to study how different microstructural factors affect D_b, D_f, and D_{FT}, and to try to find some microscopy fractal dimensions that display a similar behavior to that of the rheology fractal dimension, D_r.

MATERIALS AND METHODS

Generation of computer simulation images. This study used a program written in Matlab 6.5 from the MathWorks, Inc. (Natick, MA) to generate images with different crystal shape, size, area fraction, and distribution orderliness. Crystal shapes studied included line, diamond, square, and disk shapes; and the sizes studied ranged from around 13 to 4000 pixels. The area fraction of a crystal network was calculated by the number of pixels occupied by crystals divided by the number of pixels in the whole image, which are always 512×512 pixels in the simulation. The range of area fraction studied in the simulation was from 2 to 30%. The degree of the orderliness of a crystal network was defined as the percentage, P, of the evenly distributed crystals. The other $(1 - P)$ percentage of crystals was randomly distributed. Evenly distributed crystals were distributed in the whole image and separated by same distance in both the x and y direction. The coordinates of randomly distributed crystals were obtained by rand() function in Matlab.

Box-counting fractal dimensions calculation. Box-counting fractal dimensions D_b were calculated using the commercial software Benoit 1.3 from TruSoft Int'l Inc. (St. Petersburg, FL). The settings of the D_b calculation for simulation images (512×512 pixels) are as follows: The largest grid size is 128 pixels, the decrease coefficient is 1.3, the increasing step of rotation of grids is 15 degrees, and the total number of box size used is 18.

Particle-counting fractal dimensions calculation. The particle-counting fractal dimensions D_f were calculated using a self-written program, particleCounting.m, written in Matlab 6.5. The ROI boxes used in the calculation were from the original image to the area in the center with 35% of the original image side length. For every ROI box, the particles inside the region and on the top and left edge of the ROI box are counted. The values of the D_f of all the images submitted to the program are stored in a 1-D array, Df-half-ex, in the order of the images submitted.

Fourier-transform fractal dimensions calculation. The simulation images were transformed to their power spectrum image by applying the plug-in "Forward Fourier Transform" in Photoshop Image Processing Tool Kit 4.0 (Asheville, NC), and then the mean slope of the log-log plot between the magnitude and the frequency of the power spectrum image was calculated by the plug-in "Fourier Power Spectrum" under the pull-down menu "filters → IP Surface measurement." The Fourier transform fractal dimension, D_{FT}, is calculated from the mean slope according to Equation 7.

RESULTS AND DISCUSSION

Thousands of computer simulation images were generated by changing the shape, size, area fraction, and the distribution order of the crystals in the images. Some sample images and the microstructural factors used to generate these images are shown in Figure 2.

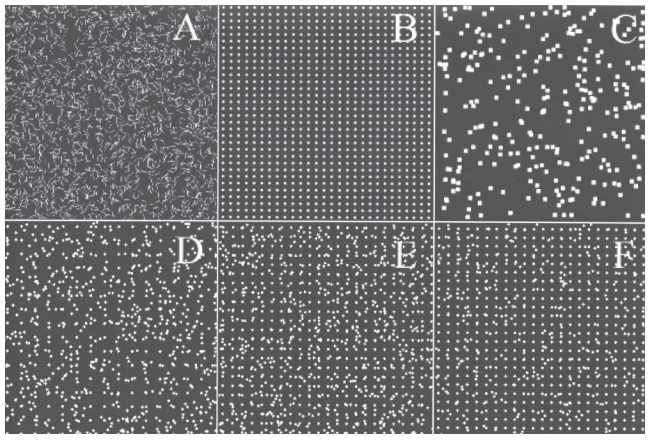

FIG. 2. Sample images generated by computer simulation. The shape, crystal size, area fraction, and the distribution orderliness for the images are (A) Line, 13 pixels, AF (area fraction) = 10%, 100% randomly distributed; (B) disk, 29 pixels, AF = 10%, 100% evenly distributed; (C) square, 49 pixels, AF = 15%, 100% randomly distributed; (D) diamond, 25 pixels, AF = 8%, 30% evenly distributed; (E) diamond, 25 pixels, AF = 10%, 50% evenly distributed; (F) diamond, 25 pixels, AF = 8%, 70% evenly distributed.

TABLE 1
D_b Values of Simulation Images with Diamond Shape and Even Distribution, but Different AF and Crystal Size[a]

Radius of crystals (pixel)	AF = 2%	AF = 6%	AF = 10%	AF = 15%	AF = 20%	Average D_b on size	SD of D_b on size
3	1.002	1.306	1.440	1.560	1.640	1.390	0.251
4	1.002	1.276	1.421	1.528	1.614	1.368	0.240
5	1.009	1.261	1.402	1.516	1.593	1.356	0.231
6	1.025	1.260	1.392	1.498	1.583	1.352	0.219
10	1.105	1.266	1.375	1.482	1.551	1.356	0.177
14	1.224	1.311	1.393	1.488	1.557	1.395	0.133
18	1.271	1.363	1.423	1.501	1.565	1.425	0.115
22	1.399	1.399	1.442	1.515	1.571	1.465	0.076
32	1.545	1.488	1.530	1.561	1.587	1.542	0.037
42	1.513	1.638	1.583	1.609	1.645	1.598	0.053
Average D_b on AF	1.210	1.357	1.440	1.526	1.591		
SD of D_b on AF	0.215	0.123	0.066	0.040	0.033	—	—

[a]AF, area fraction; D_b, box-counting fractal dimension.

By determining the D_b, D_f, and D_{FT} of these images, we studied how different microstructural factors of the fat crystal networks affected the fractal dimension values and tried to reveal the physical meaning of the D_b, D_f, and D_{FT}.

D_b was significantly ($P < 0.05$) affected by crystal shape, size, and AF (area fraction of crystals), but the distribution orderliness of the crystals had little influence on D_b. D_b increased with increasing crystal size and AF as shown by the average D_b values in Table 1. There was an interaction effect between crystal size and AF as shown by the SD of the D_b values among the simulation images in Table 1. For larger AF, the effects of crystal size on D_b became less significant, while for large crystal sizes, AF had less effect on D_b as well. These findings are consistent with the experimental results (6), where D_b was found to increase with SFC, but did not vary above a critical SFC. According to the simulation results, the increase in D_b at high SFC comes from the increased AF of the image and not from the increased number of smaller crystals. The simulation also showed that D_b is only sensitive in the low AF range, and thus low SFC range, and does not change much at higher AF, and thus high SFC. This result explains why for some polarized light microscopy of fat samples at high SFC (14), obviously different microstructures yielded similar values of D_b. The simulation also showed that line-shaped crystals always had higher D_b than block-shaped crystals, such as diamond-, disk-, and square shaped crystals.

The effects of crystal size, AF, and the distribution order on D_b are illustrated in Figures 3 and 4.

In contrast to D_b, D_f was not sensitive to crystal shape, size, area fraction, or distribution orderliness. One thing of which one needs to be aware is that the rand() function used to generate the coordinates of the crystals in images generates random numbers with uniform distribution, which means the distribution of the crystals in the images is still homogeneous. So, it is not surprisingly to see D_f was not affected by this distribution order. To study the effects of the radial distribution pattern on D_f, we generated simulation images with different density gradient of the crystals from inside to outside of the image and found that D_f is sensitive to this radial distribution pattern of the images as shown in Figure 5. Moreover, the values of D_f can exceed the dimensionality of the embedding space. This means that a particle-counting fractal dimension greater than 3 and even 4 can be obtained from 2-D images of particles distributed in space, depending on their distribution pattern. This is not the case for the box-counting dimension or the Fourier transform fractal dimension.

In Figure 6, the density of the crystals is defined as the number of crystals per 100 pixels, and the difference between the density of each ROI and the density of the most central ROI of the image was calculated as the density difference from the origin. The maximum density difference occurs between the density of the most outside ROI and that of the most inside ROI. Negative density difference values imply that there are fewer crystals per unit area in the ROI measured than the central ROI of the image, and positive values indicate there are more crystals per unit area than the central ROI. It is obvious that when $D_f < 2$, the distribution of the crystals is denser in the center and sparse in the outside of the image; whereas when $D_f > 2$, the distribution of the crystals is sparse in the center and dense in the outside of the images. In addition, the further away the D_f value is from a value of 2, the bigger the density difference of the crystals from inside to outside and the more heterogeneous the distribution of fat crystals. For instance, in Figure 6, as the

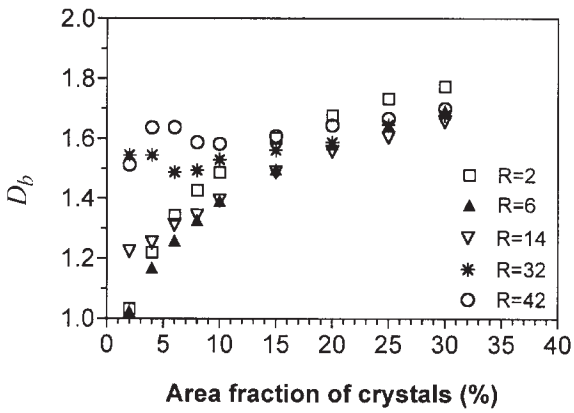

FIG. 3. The effects of AF on D_b for different crystal sizes. R is the radius of fat crystals. For abbreviations see Figures 1 and 2.

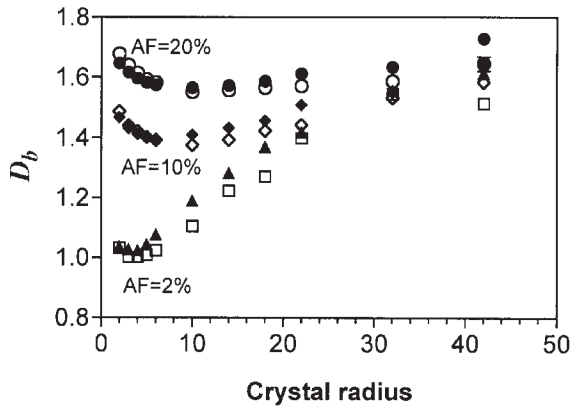

FIG. 4. The effects of crystal size on D_b. Solid symbols are for 100% randomly distributed crystals, and open symbols are for 100% evenly distributed crystals. For abbreviations see Figures 1 and 2. For explanation of symbols see Figure 3.

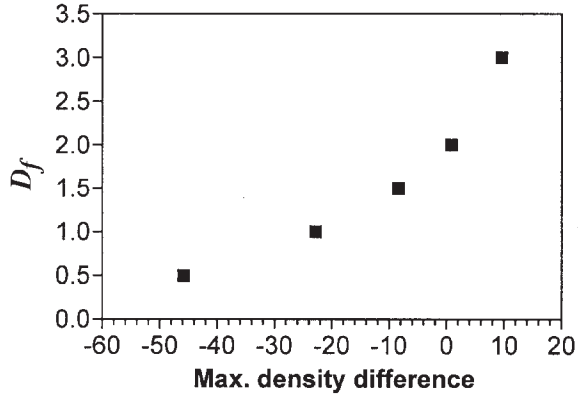

FIG. 6. D_f values of the simulation images with different maximum density difference. For abbreviation see Figure 1.

D_f increased from 2 to 3, the maximum density difference of the crystals in the image increased from 0.87 to 9.63%. The same phenomenon was observed in the experiment carried out by Campos *et al*. (15) on the crystallization of AMF and lard. The particle-counting fractal dimension of all the samples was close to 2 (and less than 2), which implied that the distributions of the fat crystals of AMF and lard were almost homogeneous. The fat samples that cooled rapidly had higher D_f, thus the distribution of the fat crystals was more homogeneous than that for fat samples cooled slowly.

The last fractal dimension studied was the Fourier transform fractal dimension D_{FT}. The study showed that D_{FT} decreases with increasing crystal size. As shown in Figure 7, D_{FT} decreased almost linearly with the radius of the crystals. The images with higher AF usually had a slightly higher D_{FT} than the images with lower crystal AF (Figs 7, 8).

Figure 8 shows that D_{FT} was only slightly affected by the area fraction and the distribution orderliness of the crystals. In general, the D_{FT} increased slightly when the AF and the distribution orderliness of the crystals were increased, but no clear trend was evident among different values for distribution orderliness at all area fractions. Relative to the effects of crystal size, the effects of distribution order and AF of the crystals on

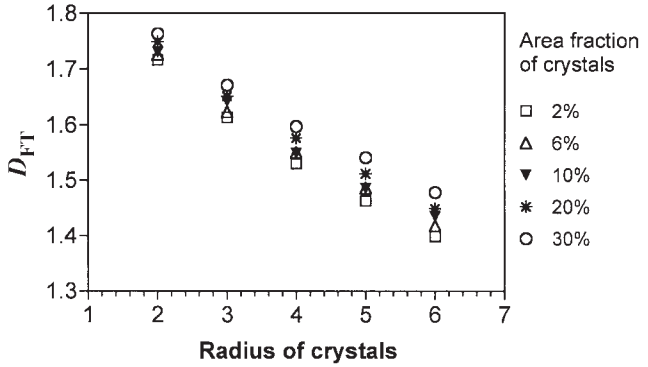

FIG. 7. Effects of crystal size and area fraction on D_{FT}. For abbreviation see Figure 1.

D_{FT} were much less significant.

Table 2 summarizes the effects of all the microstructural factors on the three microscopy fractal dimensions, D_b, D_f, and D_{FT}.

The microstructure of fat crystal networks can be quantified using box-counting, particle-counting, and Fourier transform fractal dimensions. Different fractal dimensions reflect differ-

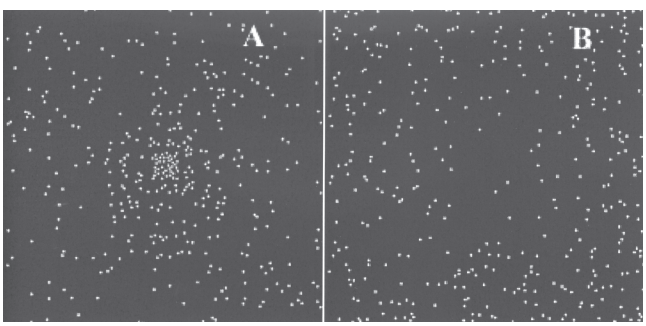

FIG. 5. Radial distribution pattern of simulation images with different D_f. (A) D_f = 0.998; (B) D_f = 3.052. For abbreviation see Figure 1.

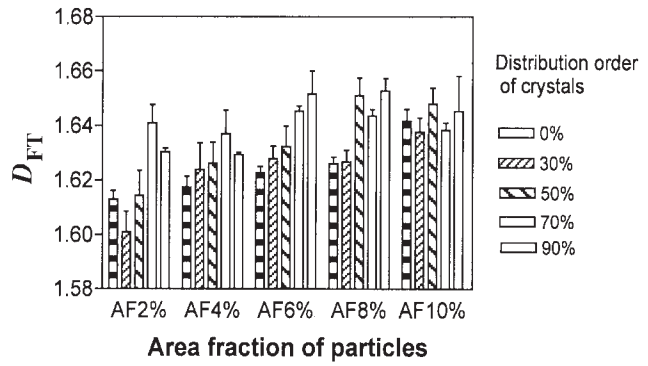

FIG. 8. Effects of area fraction and distribution orderliness on D_{FT}. For abbreviations see Figures 1 and 2.

TABLE 2
The Effects of Microstructural Factors on D_b, D_f, and D_{FT}[a]

Affecting factors	D_b	D_f	D_{FT}
Crystal shape	√	X	√
Crystal size	√	X	√
AF of crystals	√	X	X
Distribution orderliness	X	√ (radial distribution)	X

[a]D_f, particle-counting fractal dimension; D_{FT}, Fourier-transform fractal dimension; √, yes; X, no; for other abbreviations see Table 1.

ent aspects of the microstructure of the fat crystal networks and thus have different meanings. It is necessary to define which structural characteristic is most closely related to the macroscopic physical property of interest (mechanical strength, permeability, diffusion) and then use the fractal dimension that is most closely related to the particular phenomenon.

ACKNOWLEDGMENTS

The authors acknowledge the financial assistance of the Ontario Ministry of Agriculture and Food and of the Natural Sciences and Engineering Research Council. Suggestions from Dr. John Russ about part of the calculation of the Fourier transform fractal dimension were greatly appreciated.

REFERENCES

1. Marangoni, A.G., and D. Rousseau, Is Plastic Fat Rheology Governed by the Fractal Geometry of the Fat Crystal Network? *J. Am. Oil Chem. Soc. 73*:991–994 (1996).
2. Marangoni, A.G., and D. Rousseau, The Influence of Chemical Interesterification on the Physicochemical Properties of Complex Fat System. 3. Rheology and Fractality of the Crystal Network, *Ibid. 75*:1633–1636 (1998).
3. Marangoni, A.G., Elasticity of High-Volume-Fraction Aggregate Networks: A Thermodynamic Approach, *Phys. Rev. B 62*:13951–13955 (2000).
4. Narine, S.S., and A.G. Marangoni, Fractal Nature of Fat Crystal Networks, *Phys. Rev. E* 59:1908–1920 (1999).
5. Litwinenko, J.W., A.M. Rojas, L.N. Gerschenson, and A.G. Marangoni, Relationship Between Crystallization Behavior, Microstructure, and Mechanical Properties in a Palm Oil-Based Shortening, *J. Am. Oil Chem. Soc. 79*:647–654 (2002).
6. Awad, T.S., M.A. Rogers, and A.G. Marangoni, Scaling Behavior of the Elastic Modulus in Colloidal Networks of Fat Crystals, *J. Phys. Chem. B 108*:171–179 (2004).
7. Tang, D., and A.G. Marangoni, Microstructure and Fractal Analysis of Fat Crystal Networks, *J. Am. Oil Chem. Soc.*, in press.
8. Litwinenko, J.W., A.P. Singh, and A.G. Marangoni, Effects of Glycerol and Tween 60 on the Crystallization Behavior, Mechanical Properties, and Microstructure of a Plastic Fat, *Crystal Growth Design 4*:161–168 (2004).
9. Awad, T.S., and A.G. Marangoni, Comparison Between Image Analysis Methods for the Determination of the Fractal Dimensions of Fat Crystal Networks, in *Fat Crystal Networks*, edited by A.G. Marangoni, Marcel Dekker, New York, 2005, pp. 391–399.
10. Avnir D., D. Farin, and P. Pfeifer, Surface Geometric Irregularity of Particulate Materials: The Fractal Approach, *J. Colloid Interface Sci. 103*:112–123 (1985).
11. Russ, J.C., *Fractal Surfaces*, Plenum Press, New York, 1994, pp. 98–101.
12. Marangoni, A.G., The Nature of Fractality in Fat Crystal Networks, *Trends Food Sci. Technol. 13*:37–47 (2002).
13. Litwinenko, J.W., Imaging of a Model Plastic Fat System by 3-Dimensional Wide-Field Transmitted Polarized Light Microscopy and Image Deconvolution, in *Fat Crystal Networks*, edited by A.G. Marangoni, Marcel Dekker, New York, 2005, pp. 711–829.
14. Alvarado, E.D., J.N. Rodrigues, L.A. Gioielli, J.F. Toro Vazquez, and A.G. Marangoni,, Effects of Crystalline Microstructure on Oil Migration in a Semisolid Fat Matrix, *Crystal Growth Design 4*:731–736 (2004).
15. Campos, R., S.S. Narine, and A.G. Marangoni, Effect of Cooling Rate on the Structure and Mechanical Properties of Milk Fat and Lard, *Food Res. Int. 35*:971–981 (2002).

[Received November 4, 2005; accepted February 6, 2006]